In-Depth Studies of the Spectral Bandwidth of a 25 W 2 μm Band PM Hybrid Ho- and Tm-Doped Fiber Amplifier

Robert E. Tench, *Senior Member, IEEE*, Clement Romano, Jean-Marc Delavaux, Rob Lenox, Diarmuid Byrne, and Kevin Carney

***Abstract*—We report the broadband spectral performance of a three-stage, high gain, single mode, high output power (25 W) polarization-maintaining (PM) hybrid Ho-doped and Tm-doped fiber amplifier at signal wavelengths of $\lambda_s = 2004$–2108 nm. The three-stage amplifier consists of a two stage high gain Ho-doped PM single clad preamplifier stage followed by a Tm-doped PM double clad power amplifier. We employ narrow linewidth (<2 MHz), single frequency, discrete mode, packaged InGaAs/InP based laser sources to study the performance of our amplifier in a master oscillator-power amplifier (MOPA) configuration. Measurements are made over a broad wavelength range that is determined by careful selection of the properties of the Ho-doped and Tm-doped fibers in the three amplifier stages. No nonlinear effects, such as stimulated Brillouin scattering (SBS) or stimulated Raman scattering (SRS), are observed at any signal wavelength in our measurements. We compare the experimental results with steady-state simulations of both the Ho-doped preamplifier and the TDFA booster and find good agreement between data and simulations for gain, noise figure, output power, and output optical spectra.**

***Index Terms*—Doped fiber amplifiers, holmium, infrared fiber optics, optical fiber devices, polarization maintaining fiber, thulium, two microns.**

I. Introduction

NEW developments in LIDAR [1], atmospheric sensing [2], [3], and WDM transmission experiments [4]–[7] highlight the need for studies of the optical bandwidth and wavelength dependence of multi-watt, large bandwidth, high dynamic range polarization-maintaining optical amplifiers in the 2–2.1 μm band. As an example of the current state of reported devices, Engin *et al.* [8] describe a packaged two-stage single mode PM TDFA using all double-clad Tm-doped fibers with 25 W output power at first stage input signal powers of 1–5 mW (0–+7 dBm). This 2051 nm TDFA was designed with space qualified LIDAR applications as a target. No measurements of optical bandwidth, noise figure, or input signal dynamic range were given in [8]. For non-packaged devices, Goodno *et al.* [9] have presented a single mode TDFA setup yielding 608 W of output power at 2040 nm signal wavelength, also without studies of optical bandwidth or input signal dynamic range.

Recently we have demonstrated a combined single clad-double clad Tm-doped fiber amplifier with greater than 20 W single mode output and a dynamic range of >20 dB in the 2 μm band [10], and a >25W output 2 μm PM hybrid single mode HDFA/TDFA with a dynamic range of 34 dB and an estimated (but not directly measured) high output power optical bandwidth of 80 nm [11], [12]. Both demonstrations were carried out at a single input wavelength of 2051 nm.

In this paper we move our experimental and theoretical investigations to the detailed signal wavelength dependence of a PM hybrid HDFA/TDFA with a single clad Ho-doped preamplifier [13]–[21] and a double clad Tm-doped power amplifier [10]–[12]. In addition, we now extend our studies on the performance of the three stage amplifier, presenting for the first time experimental broadband results for hybrid amplification between 2004 and 2108 nm. In particular we directly measure the operating optical bandwidth of the hybrid amplifier. Comparisons of experiment with steady-state simulations of amplifier performance are also given. We find that our hybrid Ho-Tm-doped design provides a single mode PM fiber amplifier with a combination of broad operating bandwidth, large output optical signal-to-noise ratio, high input signal dynamic range, and an output power P_{out} of 28.5 W at $\lambda_s = 2069$ nm.

The structure of our paper is as follows: In Section II, we summarize the performance of the single frequency 2000 nm band semiconductor laser sources used to measure the performance of the optical amplifier. The experimental setup and architecture for our hybrid PM HDFA/TDFA is given in Section III. Section IV contains experimental and simulated results for the performance of the broadband high gain Ho-doped preamplifier. In Section V, we show the experimental and simulated performance of the full hybrid PM broadband HDFA/TDFA. Finally, Section VI discusses the results of our studies and compares our new amplifier design to previous results from the literature.

Manuscript received July 9, 2019; revised September 30, 2019 and November 19, 2019; accepted December 20, 2019. Date of publication December 24, 2019; date of current version April 15, 2020. (*Corresponding author: Robert E. Tench.*)

R. E. Tench and J.-M. Delavaux are with the Cybel LLC, Bethlehem, PA 18018 USA (e-mail: robert.tench@cybel-llc.com; jm@cybel-llc.com).

C. Romano is with the Fraunhofer IOSB, 76275 Ettlingen, Germany (e-mail: clement.romano@iosb.fraunhofer.de).

R. Lenox, D. Byrne, and K. Carney are with the Eblana Photonics, Dún Laoghaire, A96 A621, Ireland (e-mail: rob.lenox@eblanaphotonics.com; diarmuid.byrne@eblanaphotonics.com; kevin.carney@eblanaphotonics.com).

Color versions of one or more of the figures in this article are available online at http://ieeexplore.ieee.org.

Digital Object Identifier 10.1109/JLT.2019.2961987

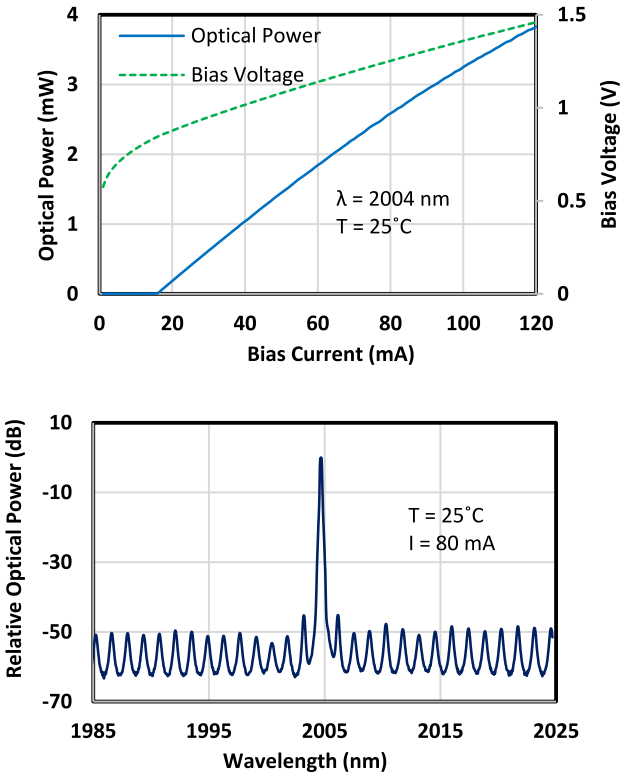

Fig. 1. Typical 2004 nm packaged DM LIV at 25 °C (top) and optical spectrum at 80 mA, 25 °C. RBW = 0.1 nm.

II. Performance of the 2000 nm Band Single Frequency Laser Sources

The 2000 nm band discrete mode (DM) laser diodes used as sources in our experiments operate over a wide temperature range with robust single frequency lasing [22]–[24]. A typical LIV curve at 25 °C and an optical spectrum at 80 mA, 25 °C for a packaged 2004 nm DM laser device are shown in Fig. 1, with typical values of threshold current of 16mA and SMSR of 43 dB. Performance of all the laser sources from 2004 to 2108 nm is comparable or better than the data in Fig. 1. Measured linewidths of the single frequency laser sources are $\leq$2 MHz.

The wavelength varies with chip temperature at a rate of 0.11 nm/°C and with a bias current tuning rate of 0.015 nm/mA, in a manner similar to the behavior of a more complex DFB laser structure. The typical stable wavelength tuning range of a 2004 nm DM laser diode is 1.2 nm at 25 °C. The output of the internally isolated laser package is a polarization maintaining fiber (Coherent/Nufern PM1950) terminated in an FC/APC connector. The optical isolation of $>$30 dB prevents feedback from interfering with the narrow linewidth operation of the laser.

The six fixed wavelength 2000 nm band DM laser devices are chosen at 2004, 2022, 2051, 2069, 2093, and 2108 nm to fully span the entire anticipated operating spectral band of the hybrid Ho-Tm doped fiber amplifier. While a tunable laser source could potentially have been used, such a source is not currently available in our laboratory. We observe that the six wavelengths chosen will present a full and complete experimental picture of fiber amplifier performance.

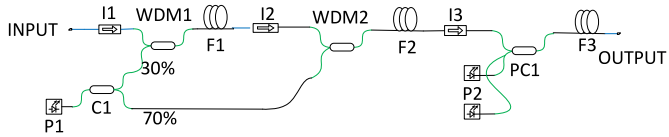

Fig. 2. Experimental setup for hybrid PM HDFA/TDFA.

We also observe that significantly higher packaged output powers of 20 mW and more can be achieved by incorporating an integrated curved tapered semiconductor optical amplifier after the DM laser structure [25].

III. Experimental Setup for Hybrid PM HDFA/TDFA

The optical design of our hybrid PM HDFA/TDFA is shown in Fig. 2. A single frequency input signal at wavelengths of 2004–2108 nm is coupled into a preamplifier consisting of two fiber stages, F1 (3.0 m) and F2 (2.0 m) of PM Ho-doped fiber, iXblue IXF-HDF-PM-8-125. Output from a multi-watt fiber laser P1 at 1941 nm is split by coupler C1 (30%/70%) and is sent to both F1 and F2 via the WDMs. The preamplifier output provides the signal input to power stage.

F3, a 6.0 m length of double clad PM Tm-doped fiber (iXblue IXF-2CF-Tm-PM-10-130). Two multimode multi-watt 793 nm laser sources from BWT Photonics are coupled into F3 by means of the 2 $\times$ 1 pump combiner PC1, to achieve the necessary high pump power of $>$50 W needed to generate $\geq$25 W of output signal power. Isolators I1—I3 suppress backward ASE, prevent self-lasing that might be caused by residual reflections, and ensure unidirectional operation of the optical amplifier. The total pump power at 1941 nm coupled into the core of F1 and F2 is designated P_{P1}, and the total pump power at 793 nm coupled into the cladding of F3 is designated P_{P2}. In our measurements, input signal power is designated as P_s and output signal power as P_{out}. P_s is measured at the input of F1 and P_{out} is measured at the output of F2 or F3 (yielding internal measurements of gain, noise figure, and input and output power). Linearly polarized signal light propagates though the fibers and components in the amplifier on the slow fiber axis.

IV. Broadband Performance of High Gain PM HDFA Preamplifier: Simulations and Experimental Results

Our approach to design simulations for the HDFA preamplifier is given in detail in [14], [15] and we present only a summary here. Table I shows the relevant physical parameters for the iXblue PM single clad Ho-doped fiber.

Simulations of single-clad Ho-doped fiber performance used the gain and absorption spectra in [15] and the data from Table I in a two-level Giles model [26] with a saturation parameter of 2.13 $\times$ 10^{18} m^{-1} s^{-1} and the addition of ion pairing. The population and propagation equations employed are described in [26] and its references. The ion pairing coefficient accounts for loss of excited state ions caused by detrimental pairwise interactions [27]–[29]. In our experiments and modeling, we chose in-band pumping with λ_p = 1941 nm, close to the peak of the fiber absorption band.

TABLE I
PARAMETERS OF SINGLE CLAD PM HO-DOPED FIBER

Parameter	Value
Fiber ID	IXF-HDF-PM-8-125
Core Diameter, microns	8
Cladding Diameter, microns	125
NA	0.15
Fiber Structure	PANDA
Birefringence	3.3×10^{-4}
Background Loss, dB/m	0.2
Peak Absorption, dB/m	57 @ 1951 nm
Ion Pairing Coefficient, %	10
$^5I_7$-$^5I_8$ Nonradiative Lifetime, mS	0.60

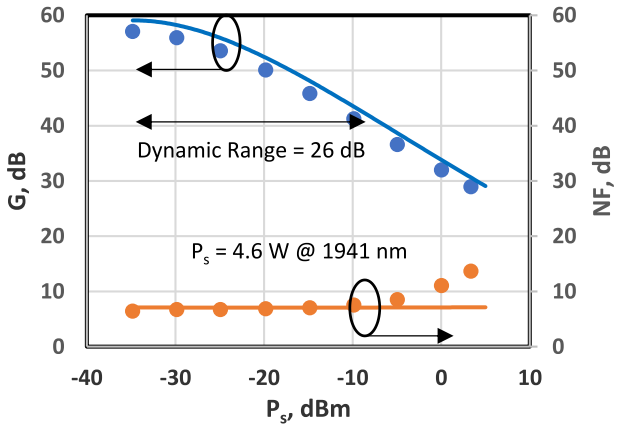

Fig. 3. Experimental and simulated G and NF vs. P_s for the Ho-doped preamplifier stage, at $\lambda_s = 2069$ nm. The points are data and the lines are simulations.

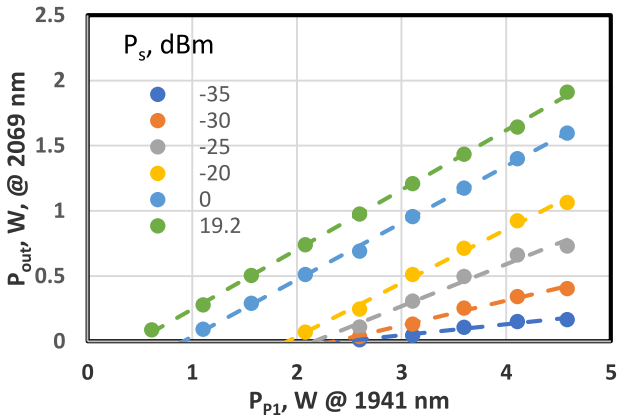

Fig. 4. P_{out} vs. P_{P1} as a function of P_s for the Ho-doped preamplifier stage. The points are data and the dashed lines are linear fits to the data.

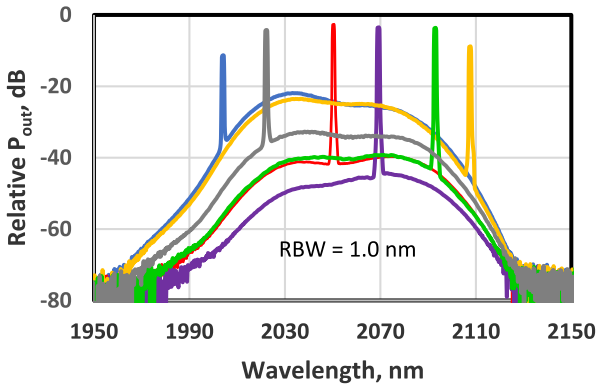

Fig. 5. Experimental output spectra for the Ho-doped preamplifier, for $P_s = -5$ dBm and $P_{P1} = 4.6$ W@ 1941 nm.

The fiber lengths $L_1 = 3.0$ m (first stage) and $L_2 = 2.0$ m (second stage) in the Ho-doped preamplifier were chosen by optimizing the first stage length for maximum simulated gain, and, subsequently, the second stage length for maximum simulated output power, for a signal wavelength of $\lambda_s = 2051$ nm and an available pump power of $P_{P1} = 4.6$ W at 1941 nm.

We begin with comparison studies of the experimental and simulated performance of the two stage PM Ho-doped preamplifier. Fig. 3 shows the experimental (points) and simulated (solid lines) values of gain G and noise figure NF for the HDFA vs. input power P_s for a signal wavelength λ_s of 2069 nm. The graph indicates that agreement between data and simulation is relatively good for G with a maximum experimental gain of 57.1 dB and a maximum simulated gain of 59.1 dB. While the functional dependence of G with P_s is predicted well by simulation, the 2 dB difference between simulation and theory for small input signals is not expected and is under active investigation. Agreement of experimental and simulated NF vs. P_s is good, with a minimum measured NF of 6.7 dB and a minimum simulated NF of 7.1 dB. The experimental NF increases for $P_s \geq -5$ dBm because a narrowband optical filter was not installed between the single frequency laser source and the input of the optical amplifier [30], and, therefore, the background broadband spontaneous emission of the laser diode creates an apparent and false increase in the measured NF value for high input powers. The measured input signal dynamic range of the preamplifier for G $\geq$ 40 dB is 26 dB as shown in Figure 3.

Fig. 4 plots the experimental variation of P_{out} vs. P_{P1} for values of P_s ranging from -35 dBm to $+19.2$ dBm at $\lambda_s = 2069$ nm. Here the points are data and the dashed lines are linear fits to the data. The highest input power of $+19.2$ dBm was achieved by using a separate PM booster amplifier (not shown in Figure 2) after the DM laser source. As illustrated by the graph, the measured output powers vary linearly with P_{P1} for all values of P_s studied. With $P_s = +19.2$ dBm, an optical-to-optical slope efficiency η (defined as $\eta = \Delta P_{out}/\Delta P_{P1}$) of 47.5% is achieved. This illustrates the good power conversion efficiency of the PM Ho-doped preamplifier. For $P_s \geq -20$ dBm, output powers of 1 W or greater are available to seed the following power amplifier stage.

In Fig. 5, we show the experimental output spectra of the amplifier for six input signal wavelengths of 2004, 2022, 2051, 2069, 2093, and 2108 nm for an input signal power of -5 dBm. For these spectra the pump power P_{P1} was set at its maximum value of 4.6 W @ 1941 nm, and the resolution bandwidth (RBW) of the optical spectrum analyzer was 1.0 nm. We observe that the maximum optical signal to noise ratio (OSNR) of 52 dB/0.1 nm is achieved at a signal wavelength of 2069 nm. The polarization

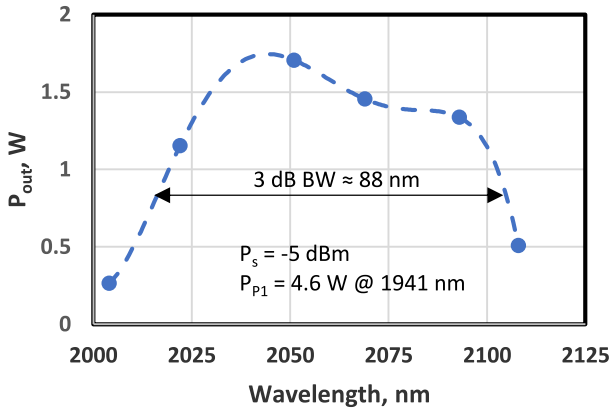

Fig. 6. Experimental saturated output power vs. λ_s for the PM HDFA preamplifier. The points are data and the dashed line is a polynomial fit to the data as a guide to the performance of the preamplifier.

extinction ratio (PER) at the output of the HDFA preamp is $\geq$20 dB [15], [16].

Comparison of our results at 2069 nm with the high gain Ho-doped fiber amplifier in [18] shows that we achieve a small signal gain of 57 dB compared to 41 dB in [18] where a double pass configuration instead of a two stage configuration is employed. Our maximum output power with a two stage configuration and 0 dBm input signal power is 1.6 W compared to the value of 0.25 W in [18]. The higher gain and larger output power result from our use of an optimized two stage configuration as well as 1.4 $\times$ higher pump power at 1940 nm.

Fig. 6, which plots saturated output power for $P_s = -5$ dBm as a function of λ_s, shows that the 3 dB (50%) output power operating bandwidth BW of the HDFA is approximately 88 nm (from 2016 to 2104 nm). Here the points are data and the dashed line is a polynomial fit to the experimental data. Since the six wavelengths chosen for the measurement are equally spaced and fully cover the operating span of the amplifier, we observe that the polynomial fit is expected to fairly represent the experimental spectral performance of the HDFA. The high OSNR and wide BW of the preamplifier make it an ideal source to seed the power amplifier, as we will see in the next section where we investigate the performance of the full three stage PM HDFA/TDFA.

The 3 dB saturated operating bandwidth of the Ho-doped fiber amplifier in [18] is estimated to be $\geq$90 nm from the spectral data presented. This agrees well with our approximate measured value of 88 nm and indicates that quite broad operating bandwidths are possible with Ho-doped fibers made with different chemical compositions and manufacturing processes.

V. Broadband Performance of the Hybrid PM HDFA/TDFA: Simulations and Experimental Results

Simulation of the double-clad TDFA under 793 nm pumping is represented using a three-level energy model ($^3H_6$, $^3F_4$, and $^3H_4$) of the thulium ion. This simplified model of the Thulium ion is based on a study of the literature; only the relevant transitions were kept. It includes the absorption, gain, and nonradiative transitions between the different levels. Ion–ion interactions

TABLE II
Parameters of Double-Clad PM Tm-Doped Fiber

Parameter	Value
Fiber ID	IXF-2CF-Tm-PM-130
Core Diameter, microns	10
Cladding Diameter, microns	125
Core NA	0.140
Outer Cladding NA	> 0.460
Birefringence	$> 0.3 \times 10^{-4}$
Cladding Background Loss, dB/m	< 0.5
Cladding Absorption, dB/m	> 6.5 @ 793 nm
Peak Core Absorption, dB/m	475 @ 1650 nm
$^3F_4$-$^3H_6$ Nonradiative Lifetime, mS	0.50

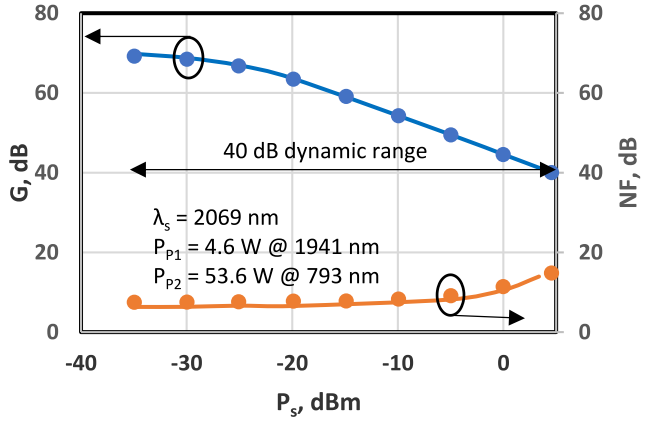

Fig. 7. Experimental and simulated G and NF at 2069 nm as a function of P_s for the hybrid HDFA/TDFA. The points are data and the lines are simulations.

are also considered: the well-known 2-for-1 effect and its opposite effect [31]. The steady-state performance simulation is achieved through solving the set of population equations and propagation equations along the active fiber [32]. The accuracy of our simulation software was demonstrated over multiple double-clad amplifier topologies using different active fibers, pumping schemes, and seed wavelength or power [33].

Parameters of the iXblue double-clad Tm-doped fiber (given in Table II) were either selected from the literature and manufacturer's data sheets as representative or measured [34] to simulate this active fiber in our software. The fiber length $L_3 = 6$ m in the Tm-doped power amplifier was chosen by maximizing the simulated hybrid HDFA/TDFA efficiency with the available 793 nm pump power and the optimized output of the preamplifier.

We begin our experimental and simulated investigations of the performance of the full hybrid HDFA/TDFA by plotting G and NF as a function of P_s for $\lambda_s = 2069$ nm. As illustrated in Figure 7, where the points are experimental data and the solid lines are simulated values, the measured small signal gain at $P_s = -35$ dBm is 69.8 dB and the simulated small signal gain is 70 dB. The excellent agreement between calculations and experiment for G is apparent from all measured values of P_s up to the maximum of +3.6 dBm. For small signal noise figure, the experimental value is 7.5 dB and the simulated value is 6.4 dB. The discrepancy between these two results is under investigation. We note that the functional dependence of NF

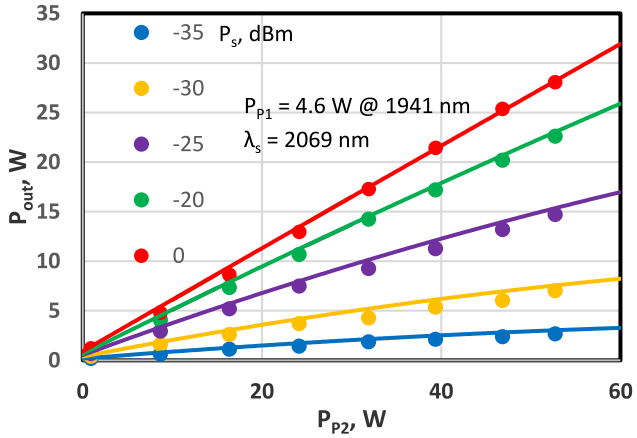

Fig. 8. Experimental and simulated P_{out} vs. P_{P2} as a function of P_s at 2069 nm for the hybrid HDFA/TDFA. The points are data and the lines are simulations.

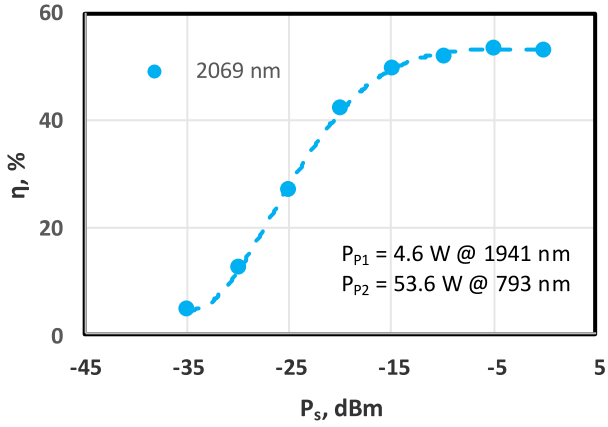

Fig. 9. Experimental optical slope efficiency vs. P_s for the hybrid HDFA/TDFA. The points are data and the dashed line is a polynomial fit to the data.

on P_s is represented quite well by the simulated values in comparison to the experimental data. As illustrated in Fig. 7, the input signal dynamic range for the amplifier is 40 dB for the criterion of $G \geq 40$ dB. Such a high value of input signal dynamic range is important in applications where the input signal power is low, e.g., for amplification of pulsed input signals with a low duty cycle.

In Fig. 8, we study another important characteristic of the hybrid HDFA/TDFA: the variation in output power P_{out} as a function of second stage pump power P_{P2} with input signal power P_s as a parameter, for $\lambda_s = 2069$ nm. Here the points are data and the solid lines are simulations. We observe that the agreement between simulation and experiment is quite good over the entire range of measured input signal powers P_s (-35 to 0 dBm) and second stage 793 nm pump powers P_{P2} (0 to 53.6 W), which validates our approach to calculating the performance of the hybrid amplifier. A maximum P_{out} of 28.5 W is experimentally observed for $P_s = 0$ dBm and $P_{P2} = 53.6$ W. No nonlinear effects, such as SBS, were observed in our measurements, as illustrated by the completely linear behavior of the output power with respect to pump power, up to the highest power levels studied. We note that this maximum observed output power is pump power limited, and we expect that output powers of 50–100 W can be readily achieved by increasing the levels of second stage pump power P_{P2}.

From the results in Fig. 8, we can calculate the optical slope efficiency of the hybrid amplifier for the maximum values of P_{P1} and P_{P2}. The optical slope efficiency is defined as $\eta = (\Delta P_{out}/\Delta P_{P2})$, and the variation of η with P_s is plotted in Fig. 9 for $\lambda_s = 2069$ nm. Here the points are data and the dashed line is a polynomial fit to the data, as a guide to the eye. As illustrated by Fig. 9, $\eta \geq 50\%$ for $P_s \geq -15$ dBm. This high asymptotic slope efficiency achieved for relatively low values of input power is caused by the high gain compression of the three-stage amplifier, a feature which is desirable for applications with low signal input powers. This behavior is also consistent with our previously reported experiments and simulations at $\lambda_s = 2051$ nm [11].

For the 25 W output power double clad TDFA in [8], an internal η of 58% is reported at 3–5 dBm internal input signal power

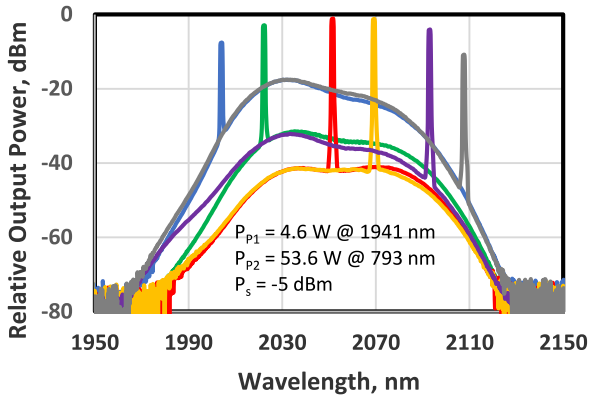

Fig. 10. Experimental optical output spectra for the hybrid HDFA/TDFA. RBW = 1.0 nm.

at 2051 nm. Our measured value of $\eta = 54\%$ at 0 dBm internal signal input power is consistent with the measurement in [8]. These results indicate that both amplifiers experience significant 2-for-1 pump to signal power conversion in the amplification process [10].

We now turn to experimental measurements of the output spectrum of the hybrid amplifier as a function of λ_s. Fig. 10 shows measured output spectra with maximum values of P_{P1} and P_{P2} and $P_s = -5$ dBm, for six values of λ_s (2004, 2022, 2051, 2069, 2093, and 2108 nm.) These spectra represent the performance of the amplifier in a highly saturated mode, and we observe that significant levels of output power are achieved for all of the measured signal wavelengths.

To investigate the measured optical bandwidth of the hybrid amplifier under saturation, we plot the peak experimental output powers from Fig. 10 in the graph of Fig. 11. Here the input signal power $P_s = -5$ dBm (yielding a fully saturated amplifier) and the pump powers P_{P1} and P_{P2} are at their maximum values. In this graph the points are data and the dashed line is a polynomial fit as a guide to the behavior of the data. As illustrated by the horizontal arrow, the measured 3 dB (50%) output power bandwidth of the amplifier is approximately 89 nm (from 2009 to 2098 nm).

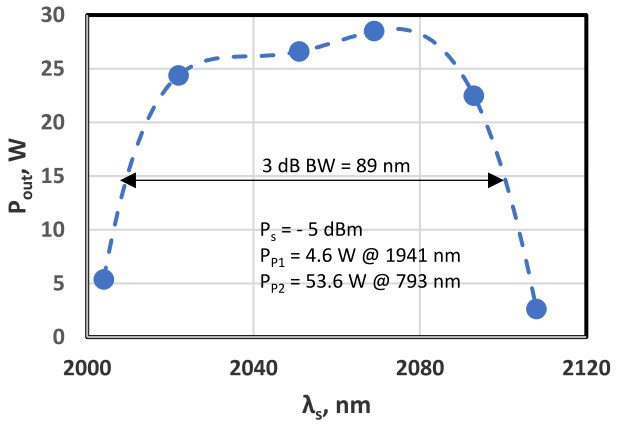

Fig. 11. Experimental saturated output power vs. wavelength for the hybrid HDFA/TDFA. The points are data and the dashed lines is a polynomial fit to the data as a guide to the performance of the hybrid amplifier.

This wide operating bandwidth is consistent with the measured spectral gain and absorption curves for the Ho-doped and Tm-doped fibers, and also agrees well with the measured output power bandwidth of approximately 88 nm for the Ho-doped preamplifier as illustrated by Fig. 4.

Preliminary measurements indicate that the PER at the output of the hybrid amplifier is $\geq$17 dB for $\lambda_s = 2069$ nm.

Our next investigation is a comparison of simulation and experiment for the output spectrum of the amplifier. We start at a signal wavelength of $\lambda_s = 2004$ nm in the low region of the amplifier's operating band, as illustrated by Figure 12(a). Here the experimental spectrum is plotted in blue and the simulated spectrum is in red. We observe that the agreement between simulation and measurement is quite good over the full wavelength range studied (1950–2150 nm) and over the full dynamic range of the data (>70 dB). Similarly good agreement is achieved for a mid-range wavelength of $\lambda_s = 2069$ nm and a high range wavelength of $\lambda_s = 2108$ nm as shown by Figures 12(b) and 12(c). For all three spectra, $P_s = -5$ dBm (fully saturated amplifier performance), $P_{P1} = 4.6$ W @ 1941 nm, and $P_{P2} = 53.6$ W @ 793 nm. The excellent match between calculation and experiment again validates our approach to simulating the performance of the hybrid HDFA/TDFA.

In Fig. 13 we show experimental (points) and simulated (solid lines) small signal G and NF as a function of λ_s, for $P_s = -35$ dBm. We find that the comparison of data and simulation is relatively good over the full wavelength range studied, with excellent agreement for G at $\lambda_s \geq 2022$ nm. For NF, the functional dependence of the data is predicted well by the simulations. This behavior indicates that the population equations, propagation equations, physical parameters, and physical assumptions discussed in Sections IV and V fairly and accurately represent the behavior of the HDFA preamplifier and the TDFA power amplifier.

The largest differences between simulation and experiment are found at $\lambda_s = 2004$ nm, a spectral region where the pump wavelength of 1941 nm for the Ho-doped fiber preamplifier is closest to the signal band of 2004–2108 nm. We discuss the context of these differences between simulation and experiment in Section VI.

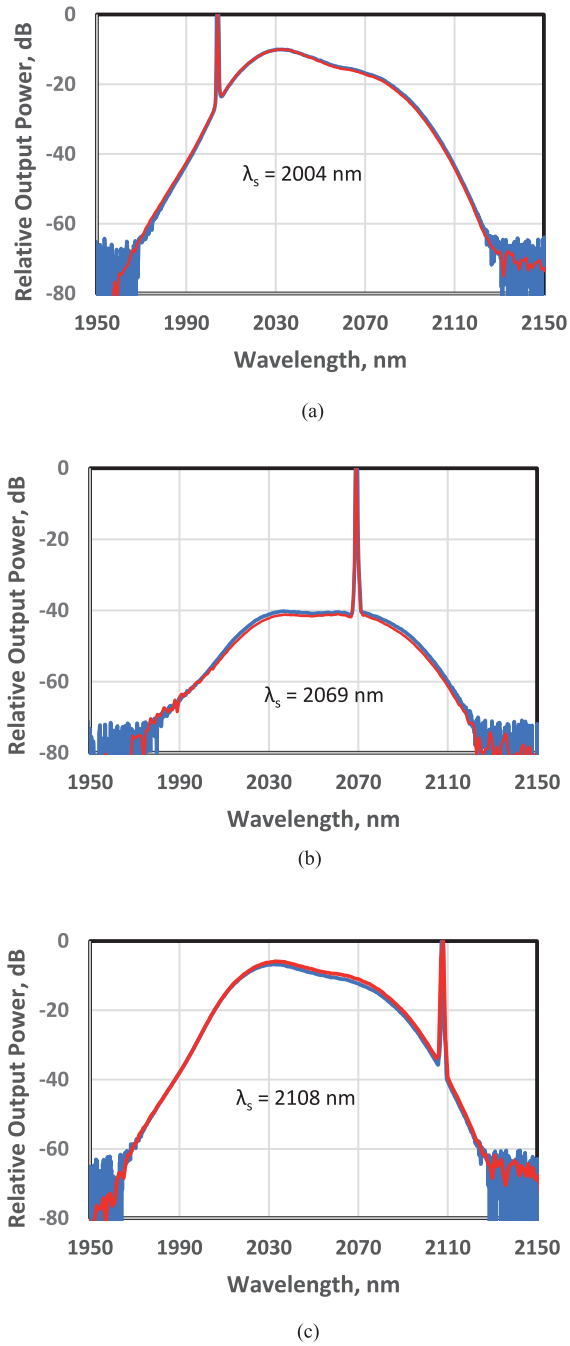

Fig. 12. (a) Simulated and experimental output spectra for $\lambda_s = 2004$ nm. RBW = 1.0 nm. (b) Simulated and experimental output spectra for $\lambda_s = 2069$ nm. RBW = 1.0 nm. (c) Simulated and experimental output spectra for $\lambda_s = 2108$ nm. RBW = 1.0 nm.

We observe that the hybrid HDFA/TDFA studied in this paper has active fiber lengths for stages F1, F2, and F3 that are optimized for a signal wavelength of 2051 nm [10], [11], [14], [15]. Because of the optimization for the middle range of possible signal wavelengths, the active fiber lengths are somewhat too long for high performance at signal wavelengths around 2004 nm, and somewhat too short for high performance

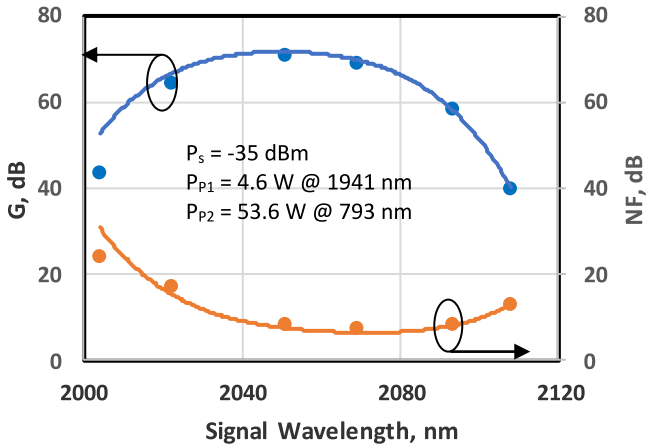

Fig. 13. Simulated and experimental small signal G and NF vs. signal wavelength for the hybrid amplifier. The points are data and the lines are simulations.

at signal wavelengths in the region of 2108 nm. Optimized operation in different wavelength bands can be accomplished by appropriately adjusting the active fiber lengths using our simulator. We note that a mid-stage wavelength bandpass filter can improve the performance of the amplifier in targeted signal wavelength regions [15].

We also observe that the output spectral band covered by the Ho-doped fiber preamplifier depends strongly on the pump wavelength chosen [18]. With our pump wavelength of 1940 nm, the operating band for the HDFA preamp roughly overlaps the operating band for the TDFA power amplifier. Increasing the HDFA pump wavelength to 2000 nm or greater, while also increasing the lengths of the active fibers in the HDFA preamp and the TDFA power amplifier, would shift the spectral operating band of the HDFA preamp and the complete hybrid HDFA/TDFA to markedly higher operating wavelengths. This is because the more completely absorbed pump light in the longer fibers would cause high wavelength spontaneous emission to build up and act as a higher wavelength secondary pump source, leading to higher wavelength emission and amplification [18]. This would enable access to higher output wavelengths with significant output powers in the region of 2130 nm.

VI. Discussion

In all of our amplifier measurements, the signal light in the 2 μm band propagates through the fibers on the slow axis. This choice was made to be consistent with standard industry practices for PM amplifiers. In the Ho-doped fiber preamplifier, the 1941 nm fiber laser pump source is polarization-maintaining, and linearly polarized pump light propagates through the HDFA preamp on the slow fiber axis. Future work will investigate the effect of orthogonal pump and signal polarizations on the performance of the Ho-doped fiber preamplifier. The second stage multimode pumps at 793 nm are coupled into the multimode cladding of the double-clad Tm-doped fiber F3 and as such do not need to be polarization maintaining.

In our studies of simulation and experiment for amplifier gain G, we observe that agreement between simulations and data for the HDFA preamp is relatively good, and that the agreement for the full HDFA/TDFA amplifier is excellent. In the case of noise figure NF, we observe some differences between the simulations and the experiments for the full hybrid HDFA/TDFA, particularly at $\lambda_s = 2004$ nm. We note that the following factors may influence the accuracy of our simulations for noise figure and gain:

1) Our gain and absorption curves for the Ho-doped fiber in the preamplifier are derived both from measurements by the manufacturer iXblue and from the literature [15], [16]. Future studies will be carried out to directly measure the gain and absorption curves for the Ho-doped fiber, to remove potential sources of uncertainty in the absorption and emission data which are currently estimated from reports in the literature and initial measurements from the manufacturer of the Ho-doped fiber. Inaccuracies here may account for the 2 dB difference observed for small signal gains in the preamplifier data shown in Fig. 3, and for the differences between simulated and experimental G and HF at 2004 nm signal wavelength for the full hybrid amplifier.
2) Our measurement of NF is carried out without a narrow bandpass filter between the semiconductor laser source and the input port of the fiber amplifier. The function of this bandpass filter is to remove the spontaneous emission background of the laser source. Future experimental studies will incorporate a narrow bandwidth optical filter to remove effects of the background of the laser source on measurements of NF for high input signal powers [30].

Simulations of P_{out} vs. P_{pump} at 2069 nm for the hybrid HDFA/TDFA show excellent agreement with the experimental data.

No stimulated scattering processes, such as SBS and SRS, are seen during the course of our measurements, as indicated by the fully linear behavior of P_{out} vs. P_{pump}. (Significant backwards Brillouin scattering would cause a significant sublinear variation in P_{out} vs. P_{pump} and no such behavior was seen.) This observation is consistent with an estimate [16] for the threshold power P_{th} of SBS for the double clad TDFA power booster of $P_{th} \geq 150$ W.

The directly measured operating bandwidth of ≈89 nm for the hybrid HDFA/TDFA agrees well with the value of 80 nm previously estimated [11] from a single wavelength measurement and also with the value of ≥90 nm for the HDFA in [18]. To our knowledge, this is the first direct experimental measurement of the operating bandwidth of a hybrid HDFA/TDFA design. Such a wide operating bandwidth is highly advantageous in a variety of applications, particularly for LIDAR and spectral sensing.

VII. Summary

In summary, we have designed and demonstrated a new and innovative broadband hybrid 2 μm band PM HDFA/TDFA consisting of a high gain, low noise figure Ho-doped fiber preamplifier with moderate output power followed by a double clad Tm-doped fiber amplifier booster stage with much higher output power. Our amplifier design exhibits high small signal

gain (70 dB), low noise figure (7.5 dB), large input signal dynamic range (40 dB), a PER of $\geq$17 dB, a wide directly measured operating bandwidth of $\approx$ 89 nm (2009–2098 nm), and a high P_{out} of 28.5 W at 2069 nm. The broadband amplifier measurements were conducted with high performance PM packaged InGaAs on InP discrete mode laser sources exhibiting 1–5 mW of fiber coupled output power and narrow linewidths of $\leq$2 MHz.

Detailed simulations of the performance of both the single clad Ho-doped fiber preamplifier and the double clad Tm-doped booster amplifier agree relatively well with the experimental data for G, NF, P_{out}, dynamic range, and optical BW. This overall agreement between simulation and data validates our approach to calculating the performance of the amplifier.

We note that the maximum output value of 28.5 W is pump power limited, and we expect that output powers of 50–100 W can readily be reached with higher power multimode 793 nm pumps in the TDFA booster stage.

Finally, our experimental demonstrations of the new amplifier architecture, combined with our validated simulations of amplifier performance, open the way for future innovative and broadband hybrid amplifier designs in the 2000 nm band for a variety of applications including LIDAR, atmospheric sensing, spectroscopy, and WDM transmission systems.

ACKNOWLEDGMENT

The authors are grateful to iXblue Photonics for the Ho- and Tm-doped fibers used in the experiments.

REFERENCES

[1] G. D. Spiers *et al.*, "Atmospheric CO_2 measurements with a 2 μm airborne laser absorption spectrometer employing coherent detection," *Appl. Opt.*, vol. 50, pp. 2098–2111, 2011.

[2] J. Caron and Y. Durand, "Operating wavelengths optimization for a spaceborne lidar measuring atmospheric CO_2," *Appl. Opt.*, vol. 48, pp. 5413–5422, 2009.

[3] J. B. Abshire *et al.*, "A lidar approach to measure CO_2 concentrations from space for the ASCENDS mission," *Proc. SPIE*, vol. 7832, 2010, Art. no. 783201.

[4] M. U. Sadiq *et al.*, "40 Gb/s WDM transmission over 1.15-km HC-PBGF using an InP-based mach-zehnder modulator at 2 μm," *J. Lightw. Technol.*, vol. 34, pp. 1706–1711, 2016.

[5] H. Zhang *et al.*, "Dense WDM transmission at 2 μm enabled by an arrayed waveguide grating," *Opt. Lett.*, vol. 40, pp. 3308–3311, 2015.

[6] H. Zhang *et al.*, "100 Gbit/s WDM transmission at 2 μm: Transmission studies in both low-loss hollow core photonic bandgap fiber and solid core fiber," *Opt. Express*, vol. 23, pp. 4946–4951, 2015.

[7] H. Zhang *et al.*, "81 Gb/s WDM transmission at 2 μm over 1.15 km of low-loss hollow core photonics bandgap fiber," in *Proc. Eur. Conf. Opt. Commun.*, Cannes, France, 2014, Paper. P.5.20.

[8] D. Engin, T. Chuang, S. Litvinovitch, and M. Storm, "Compact, highly efficient, single-frequency 25W, 2051 nm Tm fiber-based MOPA for CO_2 tracegas laser space transmitter," *Proc. SPIE*, vol. 10406, 30 Aug. 2017, Art. no. 1040606.

[9] G. D. Goodno, L. D. Book, and J. E. Rothenberg, "Low-phase-noise, single-frequency, single-mode 608 W thulium fiber amplifier," *Opt. Lett.*, vol. 34, pp. 1204–1206, 2009.

[10] C. Romano, R. E. Tench, and J-M. Delavaux, "20-W 1952-nm tandem hybrid single and double clad TDFA," *Proc. SPIE*, vol. 10512, Feb. 2018, Art. no. 105120Q.

[11] R. E. Tench, C. Romano, and J.-M. Delavaux, "A 25 W 2 μm broadband polarization-maintaining hybrid Ho- and Tm-doped fiber amplifier," *Appl. Opt.*, vol. 58, pp. 4170–4175, 2019.

[12] R. E. Tench, C. Romano, and J.-M. Delavaux, "Studies of the optical bandwidth of a 25 W 2 μm Band PM Hybrid Ho-/Tm-Doped fiber amplifier," *Proc. SPIE*, vol. 11000, Apr. 2019, Art. no. 1100009.

[13] R. E. Tench, C. Romano, J-M. Delavaux, T. Robin, B. Cadier, and A. Laurent, "Broadband high gain polarization-maintaining holmium-doped fiber amplifiers," in *Proc. Eur. Conf. Opt. Commun.*, Rome, Italy, Sep. 2018, Paper Mo3E.3.

[14] A. Hemming *et al.*, "Development of high-power Holmium-doped fibre amplifiers," *Proc. SPIE*, vol. 8961, Mar. 2014, Art. No. 89611A.

[15] R. E. Tench *et al.*, "Two-stage performance of polarization-maintaining holmium-doped fiber amplifiers," *IEEE J. Lightw. Technol.*, vol. 37, no. 4, pp. 1434–1439, Feb. 2019.

[16] R. E. Tench, C. Romano, and J.-M. Delavaux, "Shared pump two-stage polarization-maintaining holmium-doped fiber amplifier," *IEEE Photon. Technol. Lett.*, vol. 31, no. 5, pp. 357–360, Mar. 2019.

[17] S. A. Filatova, V. A. Kaminyn, V. B. Svetkov, O. I. Medvedkov, and A. S. Kurkov, "Gain spectrum of the Ho-doped fiber amplifier," *Laser Phys. Lett.*, vol. 12, 2015, Art. no. 095105.

[18] N. Simakov *et al.*, "High gain holmium-doped fibre amplifiers," *Opt. Express*, vol. 24, pp. 13946–13956, 2016.

[19] N. Simakov *et al.*, "Holmium doped fiber amplifier for optical communications at 2.05 – 2.13 μm," in *Proc. Opt. Fiber Commun. Conf. Exhib.*, 2015, Paper. Tu2C.6.

[20] A. Hemming, N. Simakov, M. Oermann, A. Carter, and J. Haub, "Record efficiency of a holmium-doped silica fibre laser," in *Proc. Conf. Lasers Electro-Optics*, 2016, Paper SM3Q.5.

[21] N. Simakov, A. Hemming, W. A. Clarkson, J. Haub, and A. Carter, "A cladding-pumped, tunable holmium doped fiber laser," *Opt. Express*, vol. 21, pp. 28415–28422, 2013.

[22] J. Patchell, D. Jones, B. Kelly, and J. O'Gorman, "Specifying the wavelength and temperature tuning range of a Fabry-Perot laser containing refractive index perturbations," *Proc. SPIE*, vol. 5825, Jun. 2005.

[23] S. O'Brien and E. P. O'Reilly, "Theory of improved spectral purity in index patterned Fabry-Perot lasers," *Appl. Phys. Lett.*, vol. 86, 2005, Art. no. 201101.

[24] R. Phelan, J. O'Carroll, D. Byrne, C. Herbert, J. Somers and B. Kelly, "In0.75Ga0.25As/InP multiple quantum-well discrete-mode laser diode emitting at 2 μm," *IEEE Photon. Technol. Lett.*, vol. 24, no. 8, pp. 652–654, Apr. 2012.

[25] R. Phelan *et al.*, "High power narrow linewidth discrete mode laser diode integrated with a curved semiconductor optical amplifier emitting at 2051 nm," *Appl. Opt.*, vol. 57, pp. E1–E5, 2018.

[26] C. R. Giles, C. A. Burrus, D. DiGiovanni, N. K. Dutta, and G. Raybon, "Characterization of erbium-doped fibers and application to modeling 980-nm and 1480-nm pumped amplifiers," *IEEE Photon. Technol. Lett.*, vol. 3, no. 4, pp. 363–365, Apr. 1991.

[27] A. S. Kurkov, E. M. Sholokhov, A. V. Marakulin, and L. A. Minashina, "Effect of active-ion concentration on holmium fibre laser efficiency," *Quantum Electron*, vol. 40, pp. 386–388, 2010.

[28] N. Simakov, "Development of components and fibres for the power scaling of pulsed holmium-doped fibre sources," Ph.D. thesis , University of Southampton, Southampton, U.K. 2017, Section 2.5.

[29] J. Wang *et al.*, "Numerical modeling of in-band pumped Ho-doped silica fiber lasers," *J. Lightw. Technol*, vol. 36, no. 24, pp. 5863–5880, Dec. 2018.

[30] D. M. Baney, P. Gallion, and R. S. Tucker, "Theory and measurement techniques for the noise figure of optical amplifiers," *Opt. Fiber Technol.*, vol. 6, pp. 122–154, 2000.

[31] G. Frith, D. G. Lancaster, and S. D. Jackson, "85 W Tm3+-doped silica fibre laser," *Electron. Lett.*, vol. 41, pp. 687–688, 2005.

[32] C. Romano, "Design of optimized thulium-doped fiber amplifiers through experiment and performance simulation," Ph.D. thesis Telecom Paris Tech, Paris, France, 2018.

[33] C. Romano, R. E. Tench, and J.-M. Delavaux, "20-W 1952-nm tandem hybrid single and double clad TDFA," *Proc. SPIE*, 2018, Art. no. 105120Q.

[34] C. Romano, R. E. Tench, and J.-M. Delavaux, "Simulation of 2 μm single clad thulium-doped silica fiber amplifiers by characterization of the 3F4–3H6 transition," *Opt. Express*, vol. 26, pp. 26080–26092, 2018.